Enzymes are proteins that catalyze (*i.e.*, increase the rate of) chemical reaction

Carbonic anhydrase

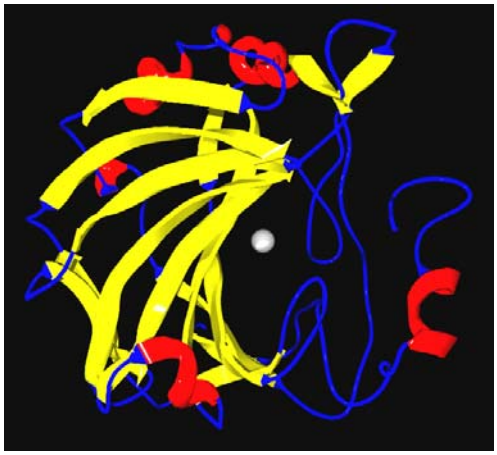

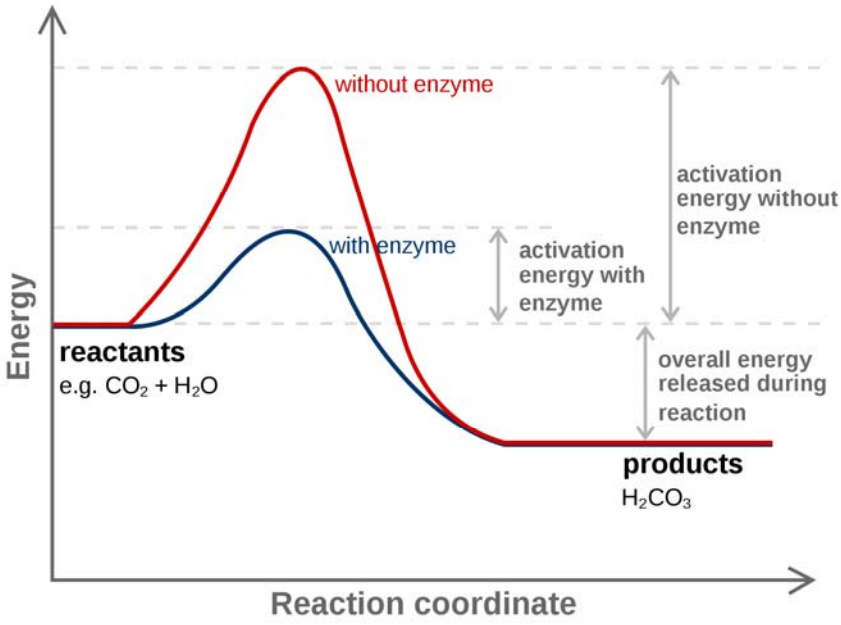

$$CO_2 + H_2O \xrightarrow{\text{Carbonic anhydrase}} H_2CO_3$$

(in tissues with high CO_2 concentration)

$$H_2CO_3 \xrightarrow{\text{Carbonic anhydrase}} CO_2 + H_2O$$

(in lungs with low CO_2 concentration)

In humans it is working nicely
Can we understand how does it work?
Increasing the rate of chemical reaction is the dream of industry

Oxidation of methane to methanol

methane

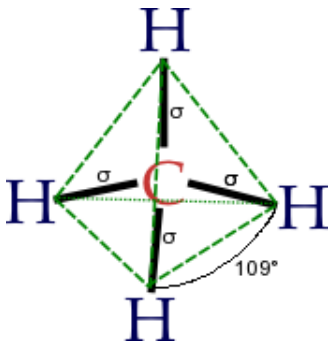

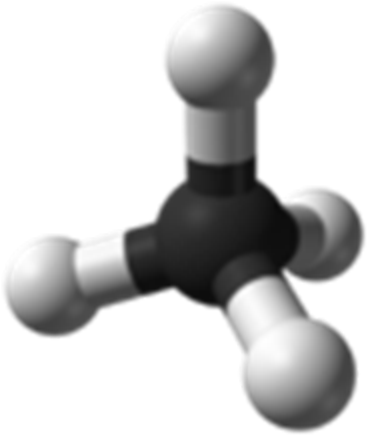

Gas
Explosive
Huge amount

methanol

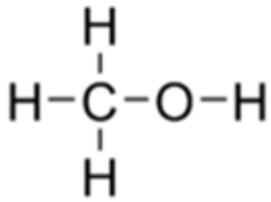

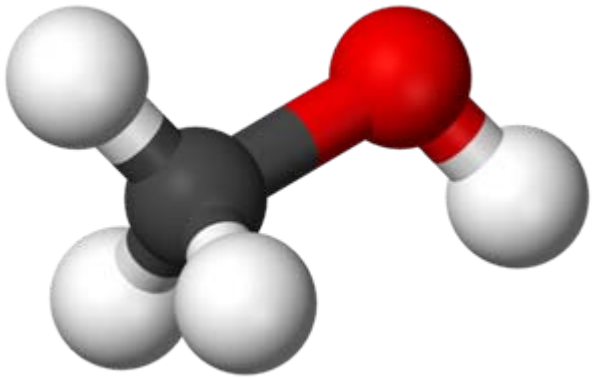

Liquid
Easy to storage
fuel

but

The methane oxidation is a difficult and expensive reaction because the methane is the most inert hydrocarbon (C-H bond is one of the most strong)

however

Methanotrophs bacteria use methane monooxygenase (MMO) enzymes to convert methane to methanol at ambient conditions !!!

monooxygenase (MMO)

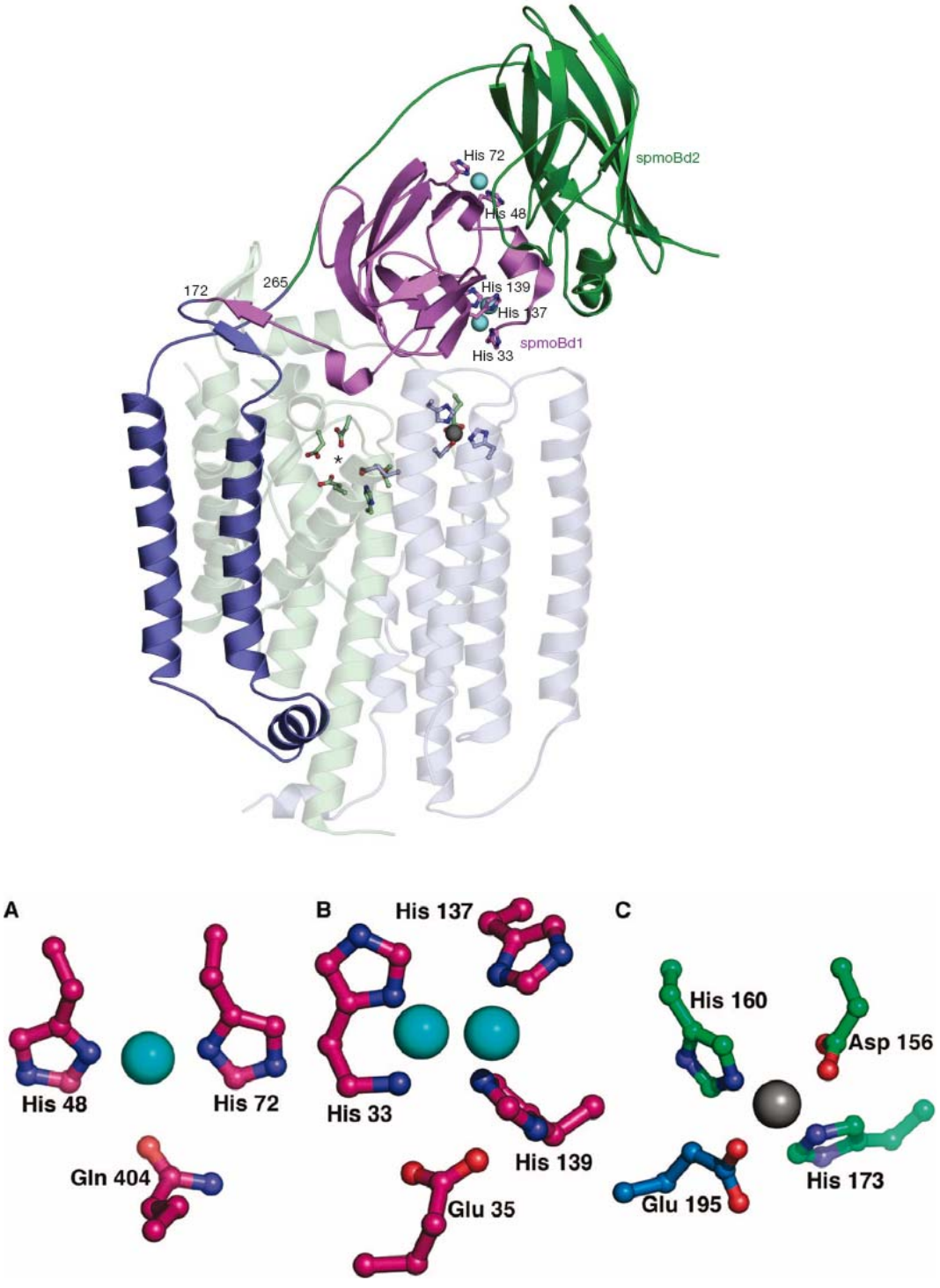

MMO metal centers. (A) Mononuclear copper center. (B) Dinuclear copper center. (C) Zinc center. Oxygen atoms are colored red; nitrogen atoms are colored blue; Zinc atom in grey

R. Balasubramanian et al., Nature **465,** 115 (2010)

Oxidation at the dinuclear copper center

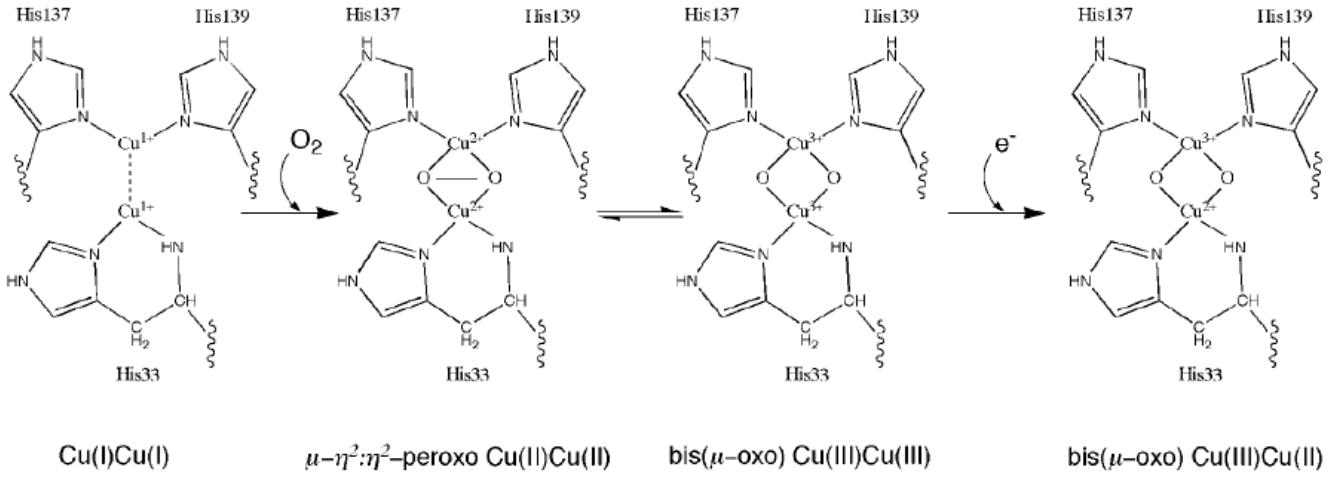

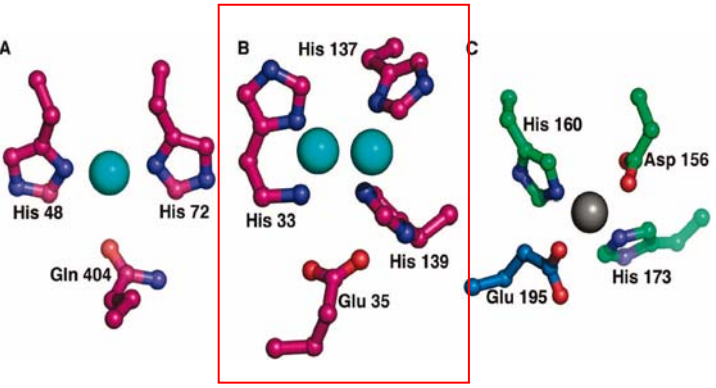

Copper edge EXAFS data and simulations for MMO

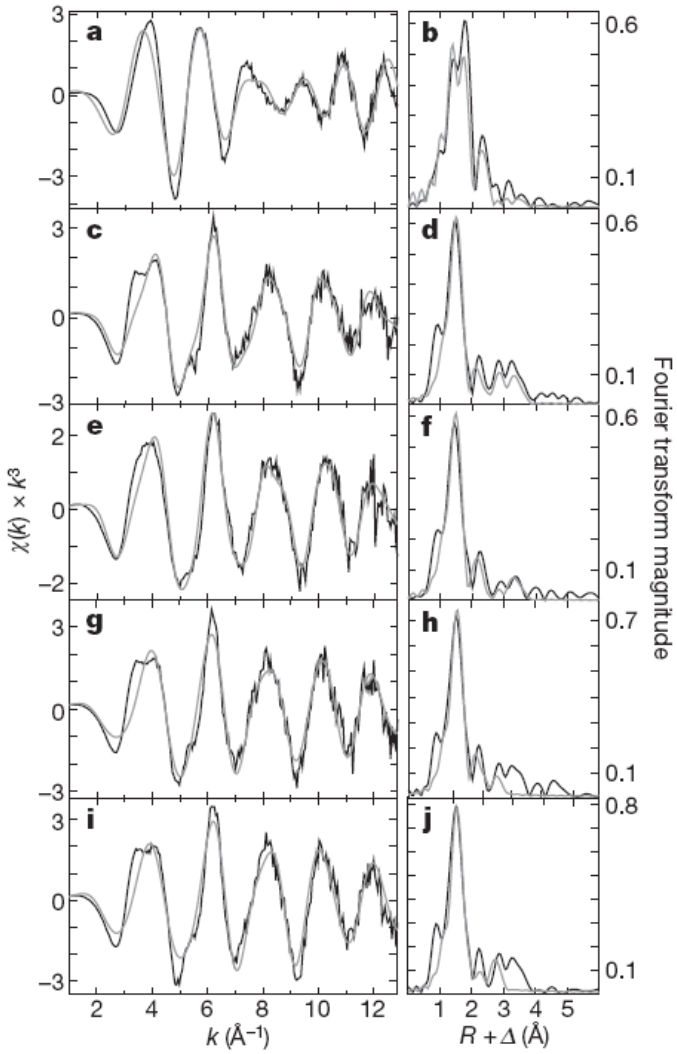

R. Balasubramanian et al., Nature **465,** 115 (2010); R. Balasubramanian et al., Acc. Chem. Res. **40**, 573 (2007)

EXAFS: Extended X-rays absorption fine structure

Principle:

1) photon in - electron out
2) The emitted electron (described by a wave) is diffused by the neighboring atoms
3) Interference between emitted and diffused wave

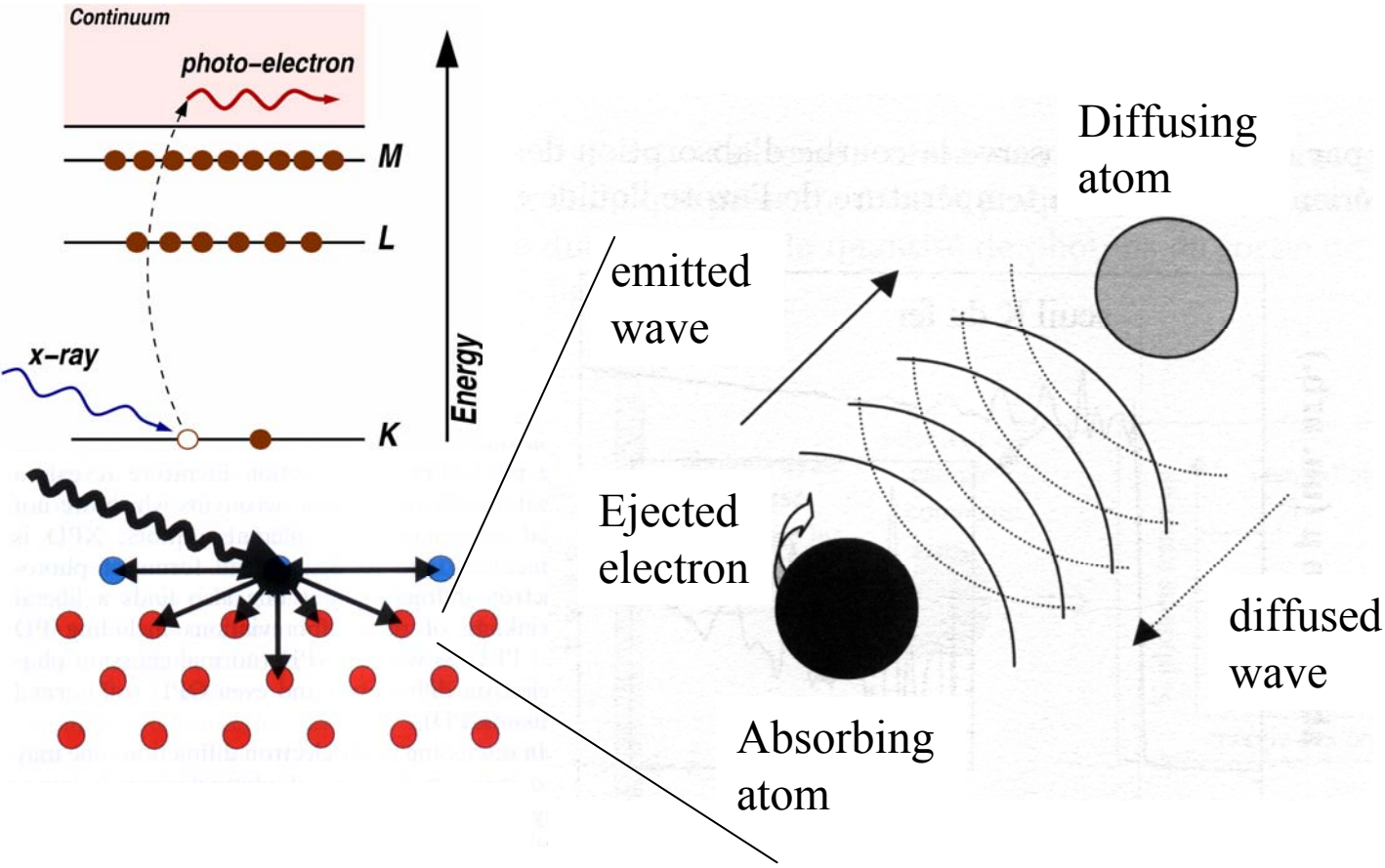

The interference between emitted and diffused wave is constructive or destructive depending on:

1) The distance between the absorbing and diffusing atoms -> sensibility to the crystallographic structure
2) The reflection coefficient of the diffusing atom -> sensibility to the chemical environment
3) The wavelength of the emitted electron -> $E_{kin} = h\nu - E_{edge} = \hbar^2k^2/2m = h^2/(2m\lambda^2)$

$\lambda = h/(2m(h\nu - E_K)^{1/2}$

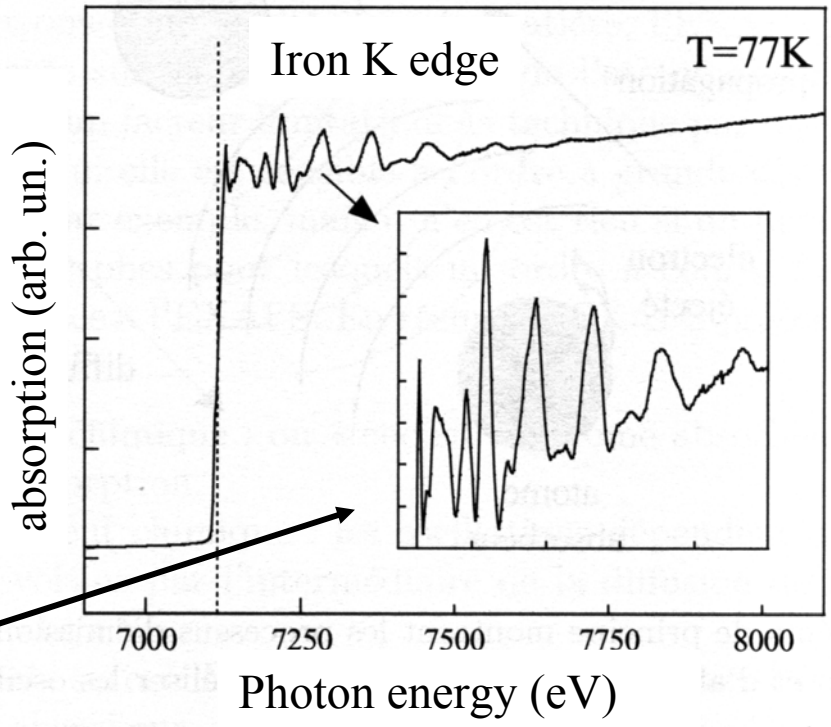

Interference conditions depend on the in-coming photons

EXAFS expression

$\chi(k) = (\mu(k) - \mu_0(k))/\mu_0(k) =$ ($\mu_0(k)$ is the atomic background)

$1/k \; \Sigma_i^{atoms} \; S_0^2 N_i(\underline{\varepsilon})/R_i^2 A_i(k) \; \exp(-2R_i/\lambda(k)) \; \exp(-2k^2\sigma_i^2) \; \sin(2kR_i + 2\delta_i + \phi_i)$

Amplitude factor

Attenuation factor: reduced electronic mean free path

Debye-Waller term: thermal vibrations and crystallographic disorder

Phase factor

kR_i -> phase due to the distance between absorbing and diffusing atom
δ_i -> phase due to the propagation in the potential of the absorbing atom
ϕ_i -> phase due to the propagation in the potential of the diffusing atom

k $\chi(k)$ is a summation over sinusoid functions

The Fourier transform of k $\chi(k)$ gives information on the phase factor or on the atomic distance

Iodine on Cu(111) *vs* bulk CuI alloy

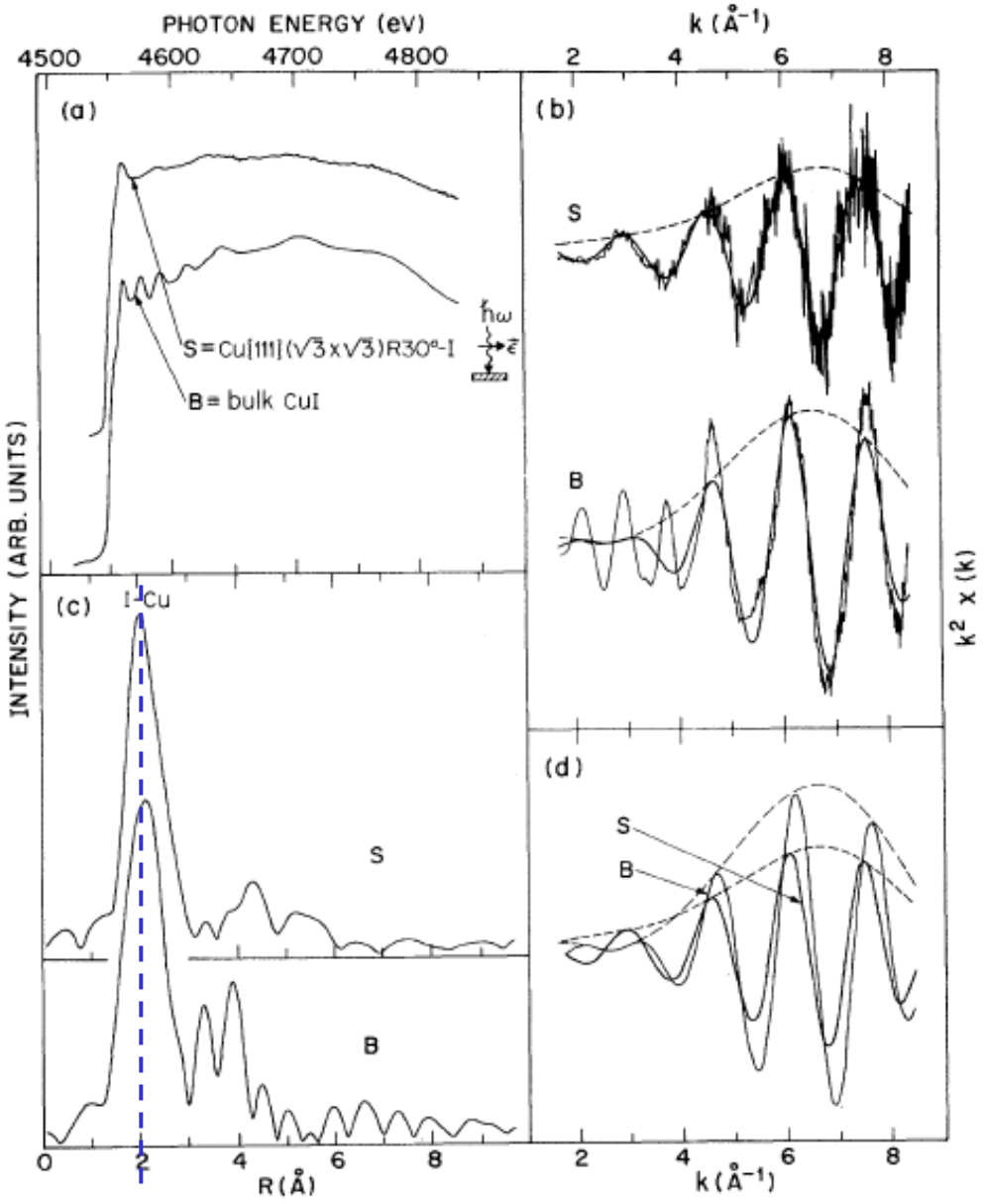

a) and b) EXAFS (at the I edge) and SEXAFS data for bulk CuI (B) and I adsorbed on Cu(111) (S); c) Fourier Transform of data in b). The double peaks for the bulk CuI are due to the I-I bonds; d) Retransformed data from c)

The Cu-I distance for the adsorbed structure is slightly shorter than in the bulk alloy

P.H. Citrin, *et al*. Phys. Rev. B **45**, 1948 (1980)

Understanding the phase-change mechanism of rewritable optical media

A. V. Kolobov, *et al.* Nat. Mater. **3**, 703 (2004).

Present interest in chalcogenide glasses is driven by the ability of a particular composition (Ge2Sb2Te5, or GST) to be repeatedly switched between crystalline (*c*) and amorphous (*a*) states by application of light or electrical pulses of suitable intensities and durations. Differences in the properties of the *a* and *c* materials (e.g., reflectivity) allows for device applications.

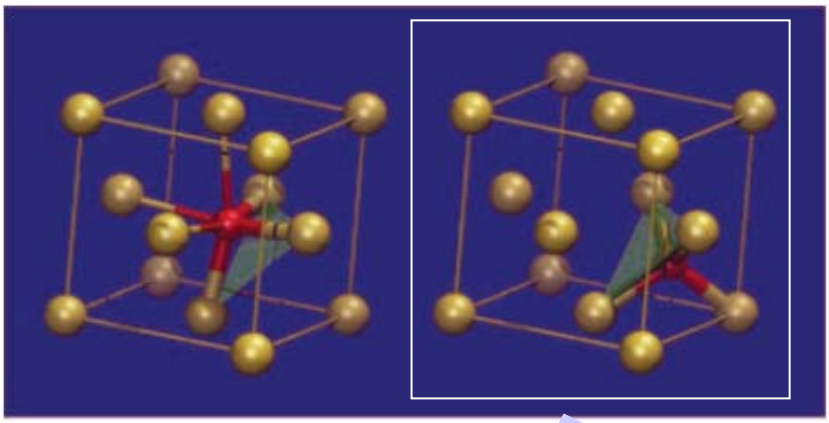

Fragments of the local structure of GST around Ge atoms in the crystalline (left) and amorphous (right) states. Stronger covalent bonds are shown as thicker lines whereas weak interblock bonds are shown as thinner lines.

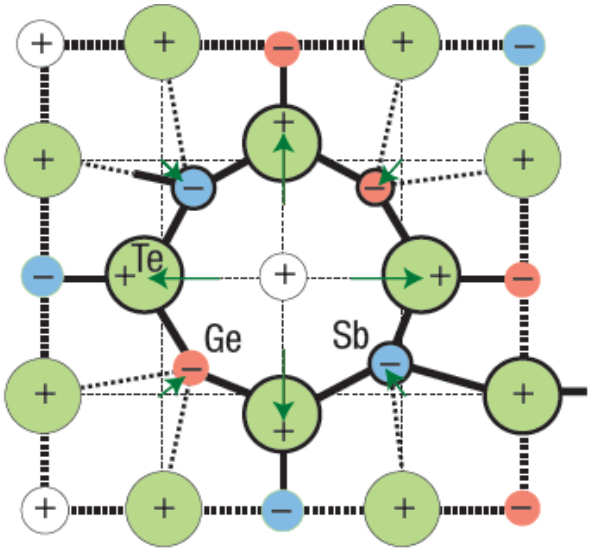

The crystal structure of laser-amorphized GST. A schematic twodimensional image of the lattice distortion of the rocksalt structure due to charge redistribution between the constituent elements; atoms that form the building block of the GST structure are shown using thick lines. The arrows indicate displacements of atoms from the ideal rocksalt positions.

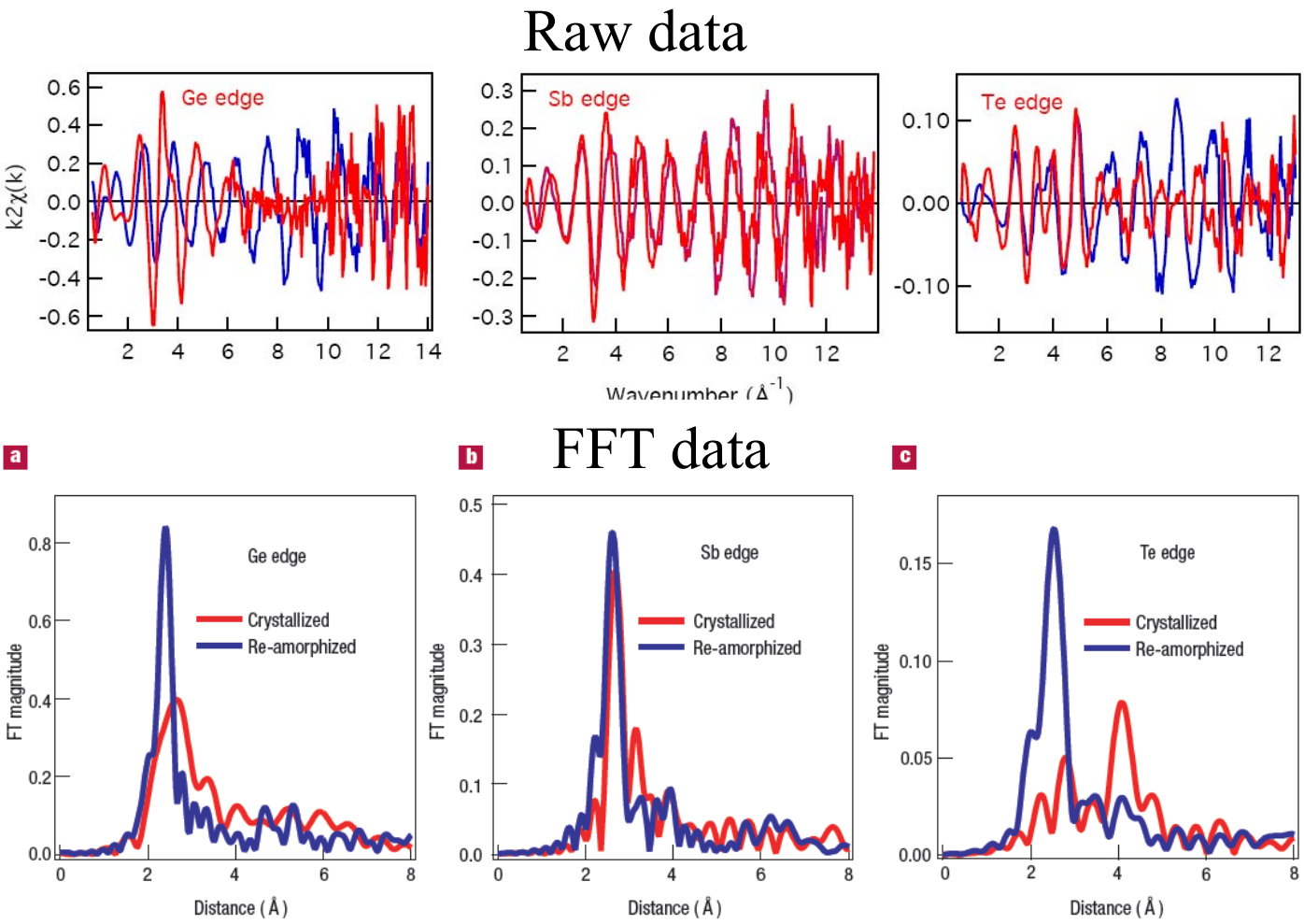

Spectra measured at the K-edges of: **a**, Ge,**b**, Sb and **c**,Te. On amorphization the bonds become shorter (as shown by shifts in the peak positions) and stronger, that is, more locally ordered (as shown by increases in the peak amplitudes and concurrent decreases in the peak widths). The peak positions are shifted from the actual interatomic distances towards lower r because of the photoelectron phase shift δ(k) in the phase factor of the EXAFS oscillations. Additionally, contributions from different nearest neighbors interfere producing extra features in the FTs.

Table 1 Comparison of the GST bond lengths determined from EXAFS and XRD analysis for the crystalline and laser-amorphized states.

Bond	Bond length (Å)	
	From EXAFS	From XRD
	Crystallized state	
Ge–Te	2.83 ± 0.01	3.0(1) ± 0.3
Sb–Te	2.91 ± 0.01	3.0(1) ± 0.3
Te–Te (2nd)	4.26 ± 0.01	4.2(6) ± 0.2
	Laser-amorphized state	
Ge–Te	2.61 ± 0.01	2.61*
Sb–Te	2.85 ± 0.01	

Polarization counts

$$N_i(\underline{\varepsilon}) = 3\,(\underline{R}_i \cdot \underline{\varepsilon})^2 / |\underline{R}_i|^2 |\underline{\varepsilon}|^2 = 3\cos^2\theta$$

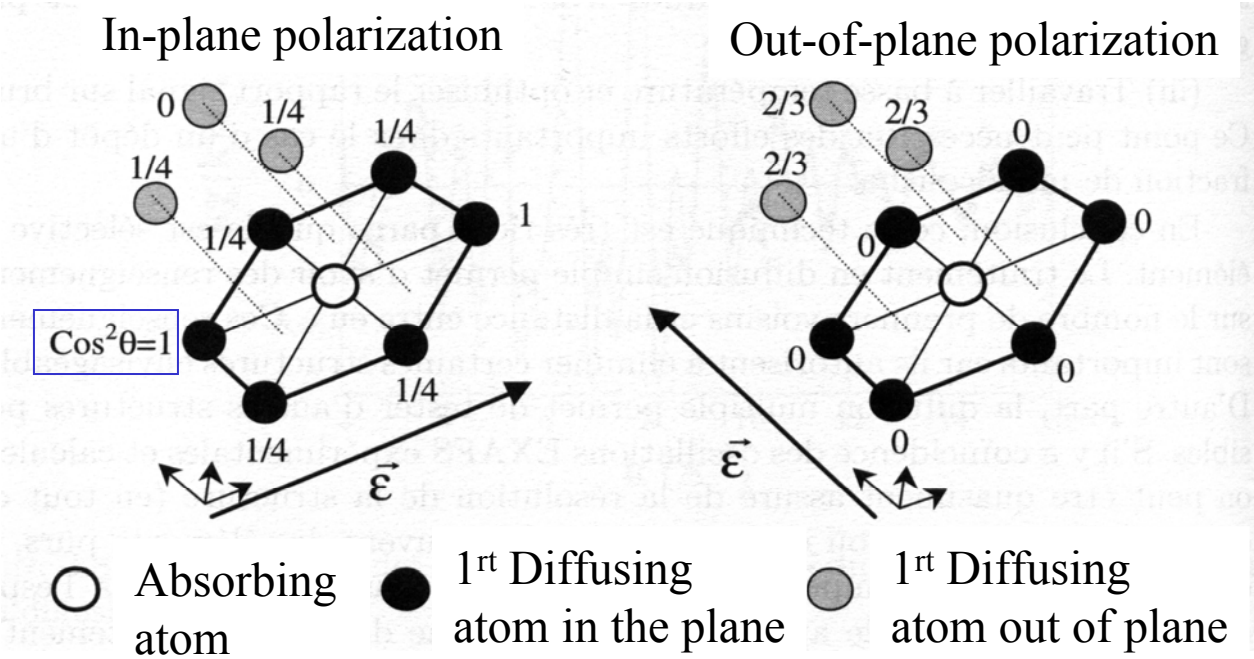

Hcp: hexagonal closed packed

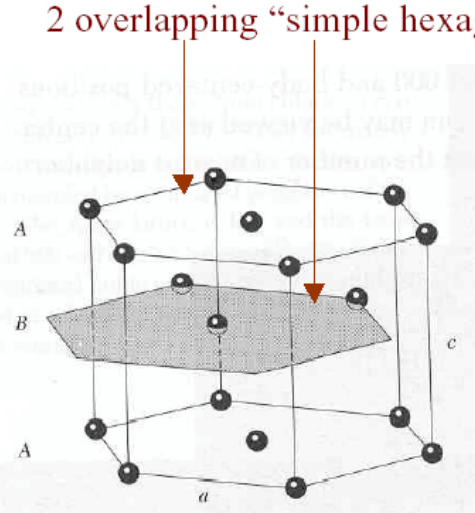

Figure 22 The hexagonal close-packed structure. The atom positions in this structure do not constitute a space lattice. The space lattice is simple hexagonal with a basis of two identical atoms associated with each lattice point. The lattice parameters a and c are indicated, where a is in the basal plane and c is the magnitude of the axis $\mathbf{a}_3$ of Fig. 14.

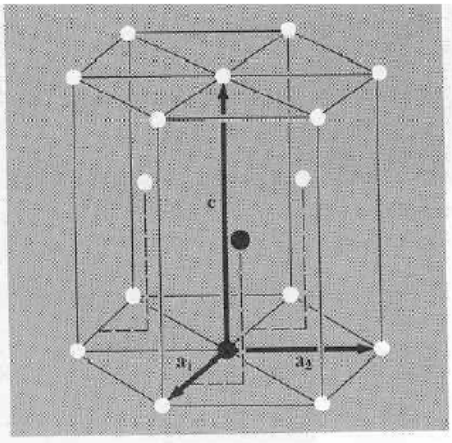

Figure 23 The primitive cell has $a_1 = a_2$, with an included angle of 120°. The c axis (or $\mathbf{a}_3$) is normal to the plane of $\mathbf{a}_1$ and $\mathbf{a}_2$. The ideal hcp structure has $c = 1.633\,a$. The two atoms of one basis are shown as solid circles. One atom of the basis is at the origin; the other atom is at $\frac{2}{3}\frac{1}{3}\frac{1}{2}$, which means at the position $\mathbf{r} = \frac{2}{3}\mathbf{a}_1 + \frac{1}{3}\mathbf{a}_2 + \frac{1}{2}\mathbf{a}_3$.

Oscillations in absorption due to *interference between outgoing and scattered photoelectrons* by neighbors at r

- Higher coordination → higher amplitude
- Shorter r → increased period

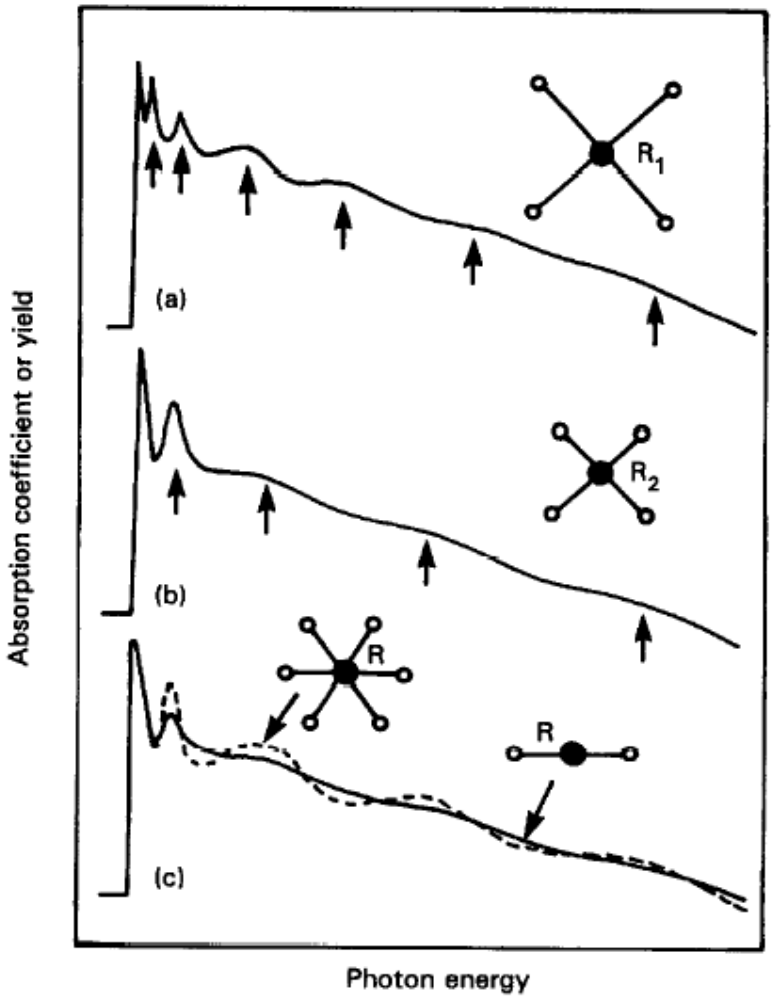

Convention:
EXAFS -> about 100 eV above absorption edge
XANES -> around the absorption edge

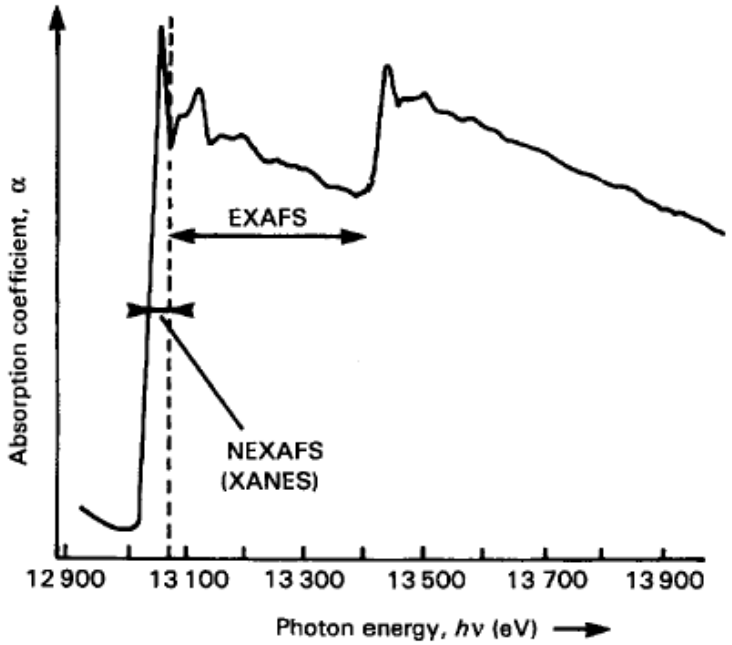

Figure 8.24. A typical X-ray absorption spectrum of a condensed medium. The sample is $BaPb_{1-x}Bi_xO_3$, and the figure shows the L_{III} absorption edge of Pb, with the NEXAFS and EXAFS regions indicated. Absorption above around 13400 eV is due to the L_{III} edge of Bi, which is close in energy to the Pb edge

Cu(110) (2x1) O

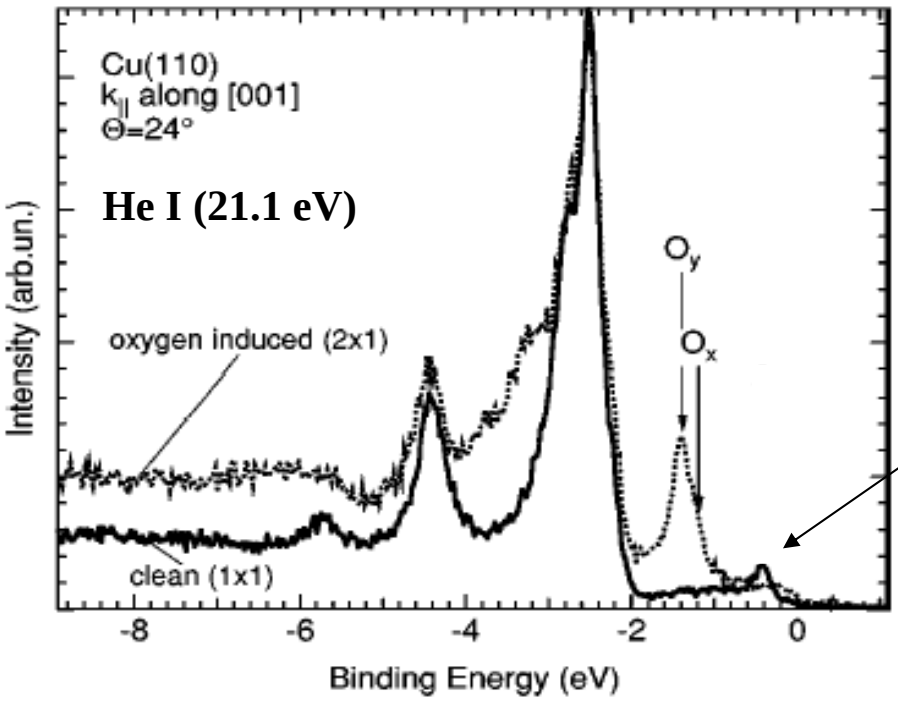

UPS spectrum

K. Stahrenberg, *et al.* Phys. Rev. B **61**, 3043 (2000).

Cu (110) Surface state

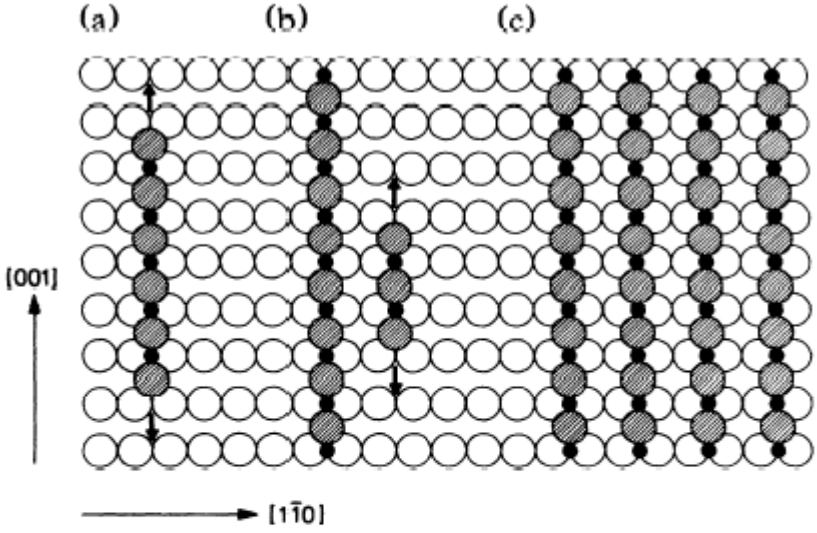

FIG. 4. Atomistic model of the different stages of (2×1)O formation. (a) Single string of Cu-O adatoms along [001] ("added row"); arrows indicate preferential growth direction. (b) Growth of a single-row (2×1)O island along [110]; nucleation of a neighbored added row. (c) Two-dimensional island of (2×1)O added-row phase, the structure being equivalent to the "missing-row" structure. Filled circles: O atoms; shaded circles: added-row Cu atoms on top of the substrate atoms (open circles).

D.J. Coulman, *et al.* Phys. Rev. Lett. **64**, 1761 (1990).

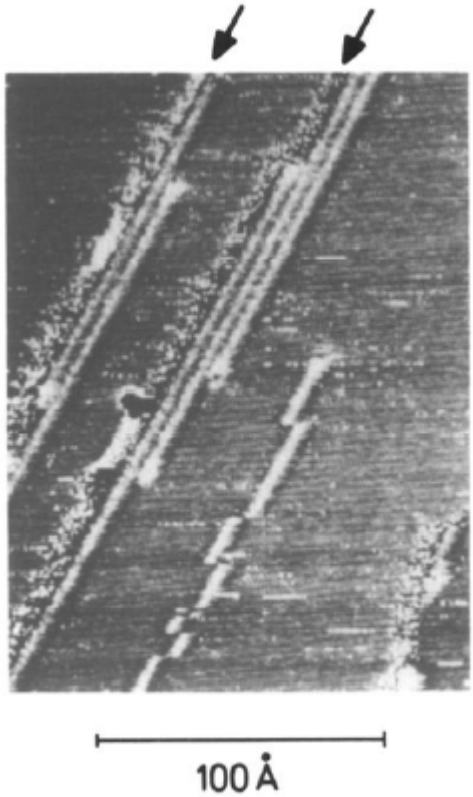

STM image of nuclei in different growth phases (step edges are marked by arrows)

Oxygen-K edges SEXAFS spectra for the Cu(110) (2x1) O at 100 K

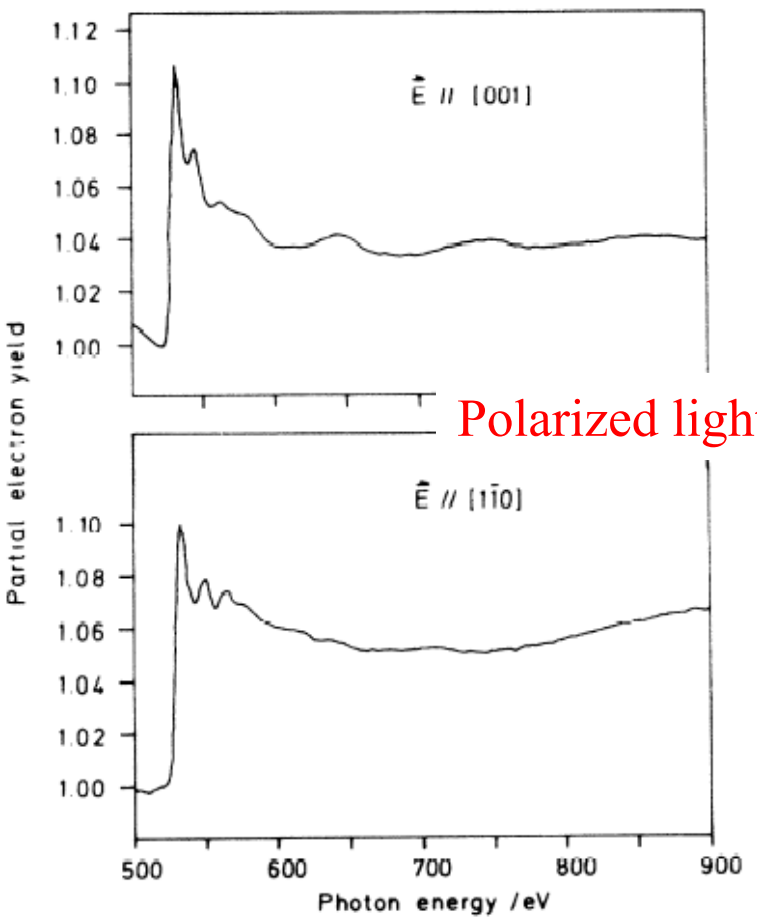

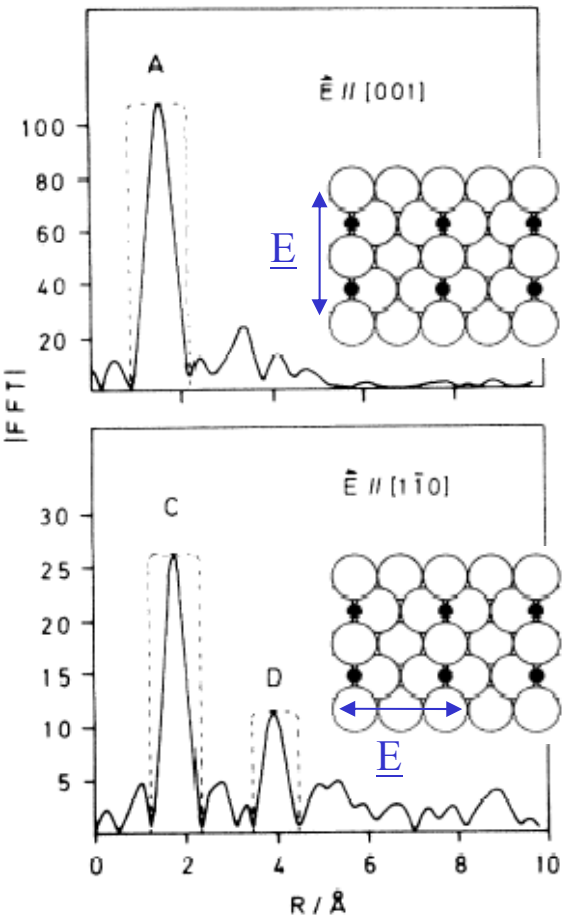

Azimuth	θ/degrees	Cu neighbor	No reconstruction	Missing row
[001]	90	1	1	1
[1$\bar{1}$0]	90	2	0.355	0.355
		3	0.458	. . .
		4	0.354	0.354

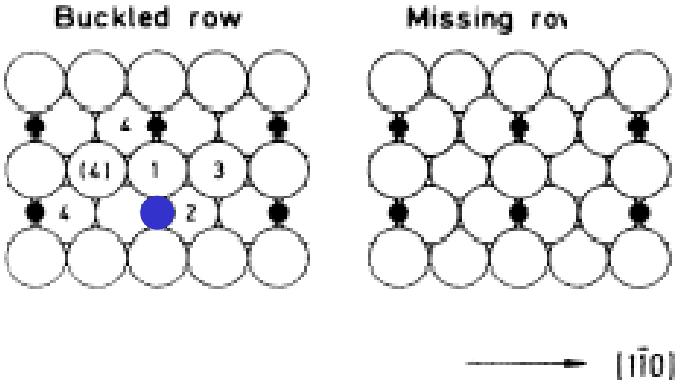

No peak due to the third neighboring is observed for E // [110] -> missing row structure

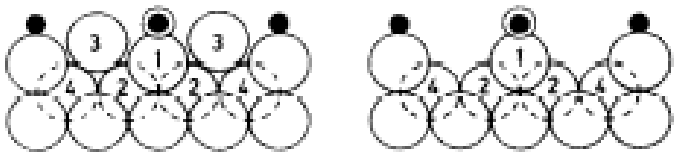

M. Bader, *et al.* Phys. Rev. Lett. **57**, 3273 (1986)

AXAFS: Atomic EXAFS

SEXAFS -> backscattering of the photoelectron at neighboring atoms

AXAFS -> scattering at the charge densities placed between the atoms.

H. Wende *et al.* Rep. Prog. Phys. **67**, 2105 (2004)

Cu(110) (2x1) O

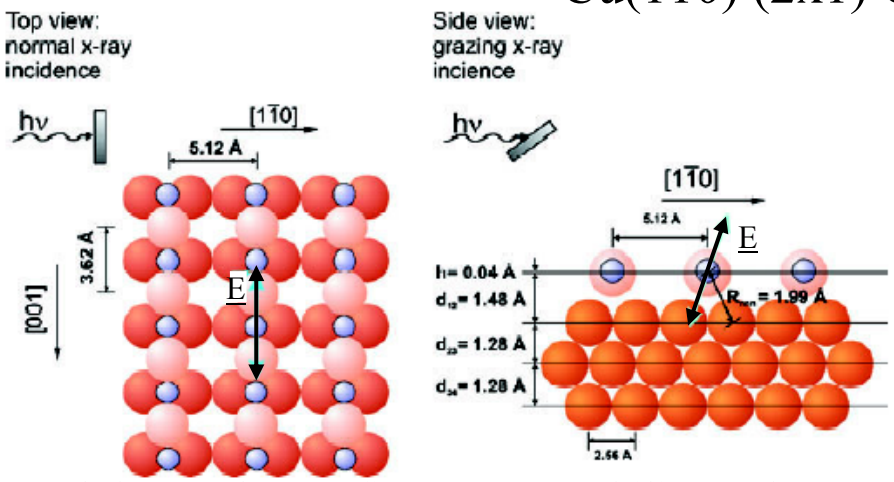

Small shaded circles: oxygen atoms, large light circles: Cu atoms of the 1rst layer, large dark circles: Cu atoms of the second and following layers. The *E*-vector for different x-ray incidences is given schematically.

Sensibility to the O - first layer Cu bond

Sensibility to the O - second layer Cu bond

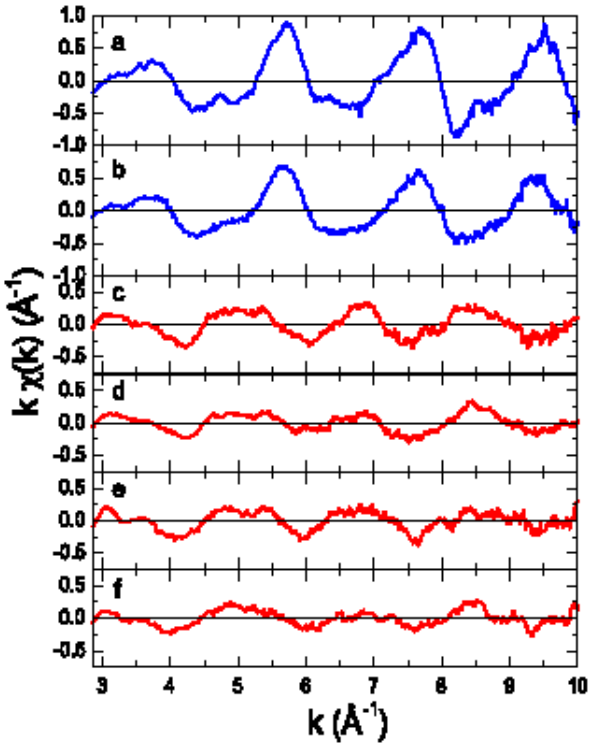

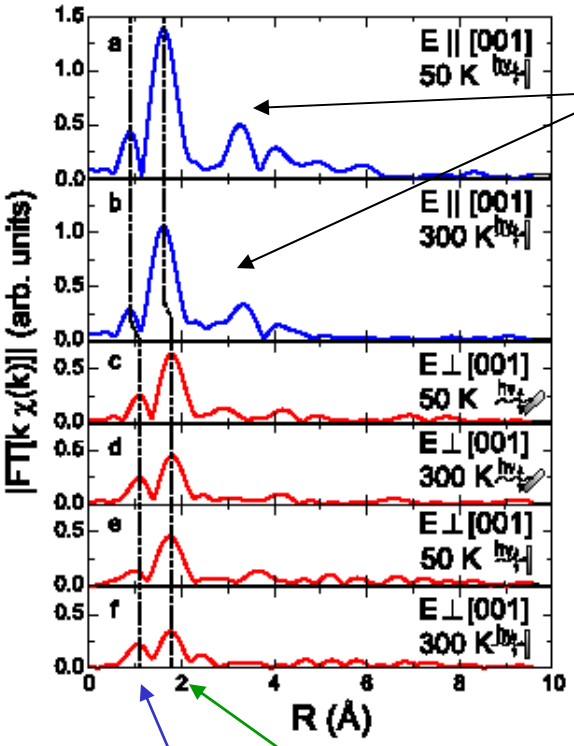

Intensity reduced at 300 K in comparison to 50 K due to the Debye-Waller term

SEXAFS nearest neighbor 1.81 ± 0.03 Å

SEXAFS next nearest neighbor 1.99 ± 0.03 Å

AXAFS nearest neighbor 0.95 ± 0.05 Å

AXAFS next nearest neighbor 1.15 ± 0.05 Å

SEXAFS

AXAFS

XANES: X-ray Absorption Near Edge Structure

The absorption edge shape is representative of the film thickness and chemical composition

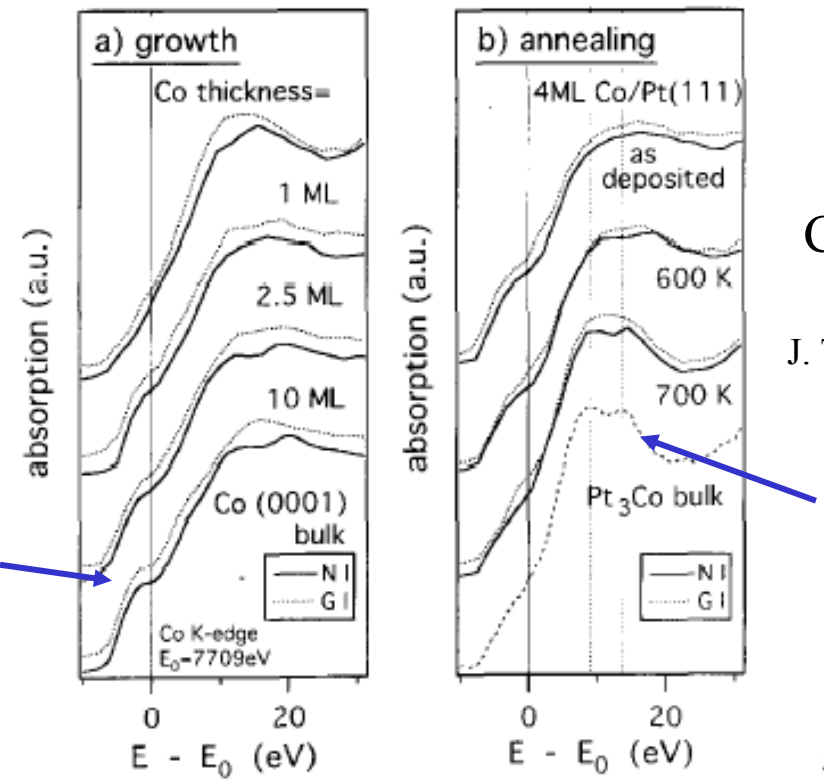

Co/Pt(111)

J. Thiele *et al.* Surf. Sci.. **384**, 120 (1997)

$SiO_2/Ni_{81}Fe_{19}$(80 Å)/Co(20 Å)/ Al(20 Å+plasma oxidation for *x* seconds)/ $Ni_{18}Fe_{19}$(100 Å)/Cu(30 Å)

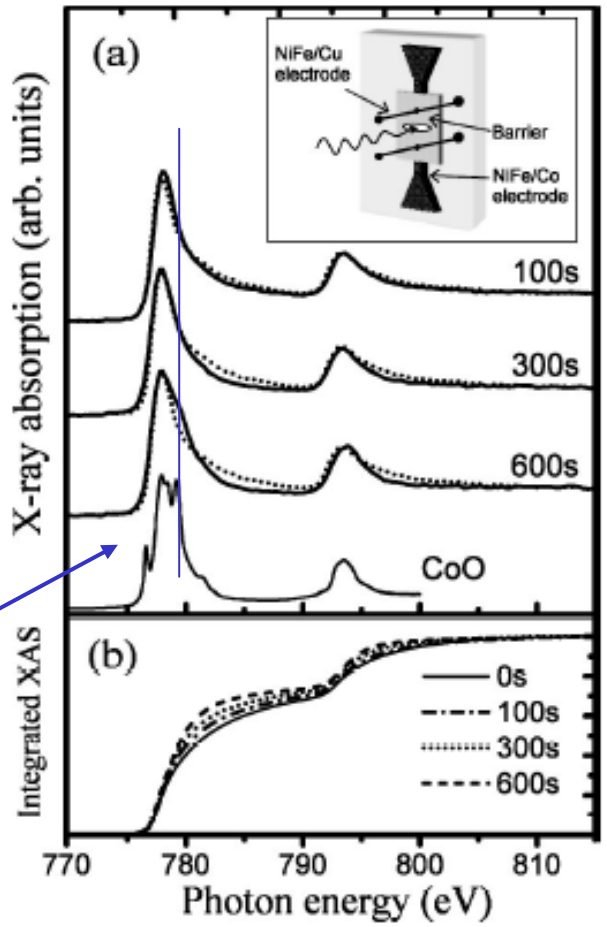

Satellite peak due to the CoO

N.D. Telling *et al.* Appl. Phys. Lett. **85**, 3803 (2004)